IEEE Access
Multidisciplinary | Rapid Review | Open Access Journal

Received July 30, 2018, accepted September 17, 2018, date of publication September 28, 2018, date of current version October 19, 2018.

Digital Object Identifier 10.1109/ACCESS.2018.2872736

Throughput Maximization in Multi-UAV Enabled Communication Systems With Difference Consideration

YU XU[1], LIN XIAO[1], DINGCHENG YANG[1], QINGQING WU[2], (Member, IEEE), AND LAURIE CUTHBERT[3]

[1]Information Engineering School, Nanchang University, Nanchang 330031, China
[2]Department of Electrical and Computer Engineering, National University of Singapore, Singapore 117576
[3]Information Systems Research Centre, Macao Polytechnic Institute, Macau 999078, China

Corresponding author: Lin Xiao (xiaolin@ncu.edu.cn)

This work was supported in part by the National Natural Science Foundation of China under Grant 61703197, Grant 61561032, and Grant 61461029, in part by the Jiangxi Postdoctoral Science Foundation Funded Project under Grant 2014MT561879 and Grant 2014KY046, in part by the Young Scientists Project Funding of Jiangxi Province under Grant 20153BCB23020 and Grant 20162BCB23010, and in part by the Natural Science Foundation of Jiangxi Province under Grant 20161BAB202043 and Grant 20114ACE00200.

ABSTRACT This paper investigates a UAV-enabled wireless communication system with multiple UAVs (multi-UAVs), where the UAVs are dispatched to collect information from a group of ground terminals (GTs) that are energy-constrained. In particular, we consider that UAVs may differ so that each UAV can be individually designed. Besides, for the sake of collision avoidance of these multi-UAVs, an effective security flight mechanism is designed. To achieve a fair performance between GTs, this paper aims to maximize the minimum GT throughput by jointly optimizing the communication scheduling, power allocation, and UAVs' trajectories. However, the formulated problem is shown to be a mixed integer non-convex optimization problem that is hard to solve. To tackle this problem, we first decompose it into two subproblems, and then, an efficient iterative algorithm is proposed by applying the block coordinate descent, relaxation, as well as successive convex optimization techniques. The proposed algorithm can be effectively utilized in wireless communication and networks. Moreover, a benchmark is set for the purpose of illustrating the superiority of the proposed design. Finally, numerical results show that the proposed design achieves a significant performance gain as compared with the benchmark.

INDEX TERMS UAV communications, throughput maximization, power allocation, flight plan design, non-convex optimization.

I. INTRODUCTION

Recently, unmanned aerial vehicles (UAVs, also known as drones) have attracted increasing attention as they offer cost reduction and new applications such as in cargo delivery, communication platform, surveillance and monitoring, search and rescue [1]–[3]. From [1], we know that small UAVs (typically with weight not exceeding 25 kg) are easily accessible to the public in several applications including wireless communication. Compared to traditional terrestrial communication systems, UAVs can be deployed swiftly and reconfigured flexibly due to the controllable mobility in three-dimensional (3D) space. In addition, in low-altitude UAV wireless communication systems, the channel between ground terminals (GTs) and UAV is highly likely to be a line-of-sight (LoS) link. Thus, UAVs can effectively assist communication coverage and capacity enhancement for the existing wireless communication networks as well as play an important role in many scenarios, such as traffic offloading, mobile relaying, wireless energy transfer, information broadcasting and data collection [4]–[7]. In practice, the flight behaviors and flight profiles of UAVs are different. In general, UAV is categorized into two types, i.e., fixed-wing UAV and rotary-wing-UAV, each with its own advantages and limitations. Without loss of generality, we can summarize UAV types and compare their performance in Table 1 based on [1], [8], and [9].

A. EXISTING WORKS AND ANALYSES

In UAV-enabled wireless communication systems, the deployment/placement of a UAV is expected to produce the

TABLE 1. UAV types and performance comparison.

Types	Advantages	Limitations	Mission Speed (Miles/hour)	Mission Radius (Miles)	Mission Endurance (Hours)
Fixed-wing UAV	Higher payload, higher speed	Need to maintain forward motion	10-75	5-25	1-4
Rotary-wing UAV	Can hover and take off and land vertically	Lower payload and lower speed, shorter range	0-40	0-8	1/6-1

best wireless coverage by optimizing its altitude and horizontal position [10]–[15]. In particular, the work in [11] analyzed a novel emergency UAV deployment and aimed to minimize the UAV deployment delay. In [12], Zeng *et al.* provided an analytical approach to minimize the number of mobile base stations mounted on UAVs to provide wireless coverage for a group of distributed GTs. In [14], the efficient deployment of multiple UAVs in downlink scenario was analyzed. In fact, the trajectory of a UAV can be optimized over time to greatly improve the communication performance [16]. Motivated by this, Xie *et al.* [6] investigated a UAV-enabled wireless powered communication network (WPCN) in which a UAV is dispatched to charge ground users via wireless power transfer, and simultaneously collects the information transmitted by the users using the harvested energy. The work in [17] analyzed the power control problem of UAV-supported ultra-dense networks with four representative scenarios. In addition, the prior work [18] developed an energy-efficient relaying scheme, but the trajectory of the UAV is predetermined. Mozaffari *et al.* [19] investigated a UAV acting as a flying base station in a device-to-device (D2D) communication network, while the UAV is only allowed to communicate at the specified points. As a result, the UAV's mobility in [18] and [19] is not fully exploited. To fully exploit a UAV's mobility, a joint trajectory optimization and communication design is considered in [20], where the UAV's mobility is continuously optimized over the period. Wu and Zhang [21] further studied both delay-constrained and delay-tolerant services of a UAV by taking into account the heterogenous user delay requirements, and the proposed problem of minimum average throughput maximization was tackled via the UAV flight plan design and OFDMA resource allocation.

However, the existing work in the literature on UAV-enabled communication systems mainly focuses on a single UAV, although there is some works that studied multiple UAVs (multi-UAV) applied in many scenarios (e.g., [20], [22]–[24]). Specifically, it is worth mentioning that [20] investigated a multi-UAV enabled multiuser system in which the UAVs act as aerial base stations to serve ground users. The work in [22] investigated teams of UAVs that are used for fighting forest fire. Considering the limited payload of UAVs, Horiuchi *et al.* [23] proposed a multi-UAV cooperation system for long distance real-time data transmission. In [24], the coverage probability of multiple UAVs was studied and the optimal altitude of UAVs obtained. However, those existing research achievements on multi-UAV do not involve the difference consideration of UAVs. For multi-UAV communication systems, it is necessary to take account of the difference of UAVs if there are different types, size, weight, and power (SWAP) constraints and communication performance among the UAVs. Besides, in some cases, the task allocation for UAVs also needs to be individually designed to meet the requirement of the networks, especially for the heterogeneous communication networks. As a result, based on the above discussion, multi-UAV communication system design with difference consideration is a promising and practical topic that can greatly improve the performance of multi-UAV communication networks.

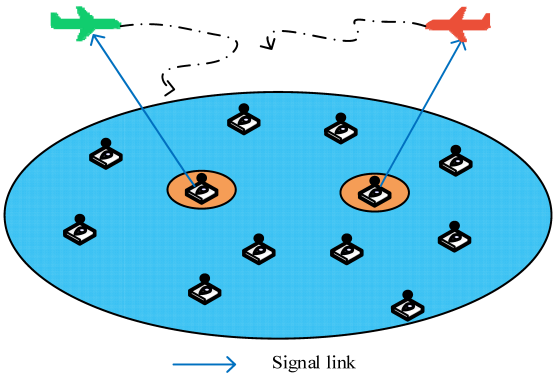

FIGURE 1. Multi-UAV enabled wireless communication system with difference consideration.

B. CONTRIBUTIONS OF THIS PAPER

In this paper, a new multi-UAV enabled communication system is studied, as shown in Fig. 1, where the difference of the UAVs is taken into consideration. In this system, multiple UAVs are dispatched to collect information from a group of GTs that are randomly distributed across the geographical area. It is assumed that these UAVs take turns to collect the data from their served GTs using time-division multiple access (TDMA). In addition, there is only one UAV-GT communication pair at most that can be linked at any time instant. Thus, by using this communication protocol, the co-channel interference caused by UAV-GT pairs can be effectively avoided. Note that our work is also suitable for downlink communication, such as information broadcast systems. In order to be in accord with reality, each GT's energy for communication is assumed to be limited, and the transmission power at any time instant is subject to a maximum instantaneous power constraint. Note that in the proposed system, one of the major problems is the communication scheduling for multiple UAVs as well as GTs during the period time. Intuitively, a UAV would select one associated GT that is in a better GT-to-UAV channel. Next, the UAV would fly closer to the associated GT and even hover over

it for an optimal link. In this paper, our objective is to maximize the minimum GT throughput, which leads to a new design framework needed to jointly consider the communication scheduling, power allocation and trajectory optimization. To the best of our knowledge, multi-UAV communication systems with difference consideration of UAVs has not been studied in the literature.

C. ORGANIZATION AND NOTATIONS

The rest of this paper is organized as follows. Section II presents the system model and the problem formulation for a multi-UAV enabled communication system. In Section III, an effective iterative algorithm for solving the formulated problem is proposed. The numerical results are presented in Section IV to demonstrate our proposed design. Finally, the main conclusions of this paper are summarized in Section V.

Notations: In this paper, italic letters are used to denote scalars, while vectors and matrices are respectively denoted by bold-face lower-case and upper-case letters. Moreover, $\mathbb{R}^{M\times 1}$ denotes the space of M-dimensional real-valued vector. $\|\mathbf{a}\|$ represents the Euclidean norm of vector $\mathbf{a}$, and $|\mathcal{K}|$ denotes the cardinality of set $\mathcal{K}$. For a time-dependent function $y(t)$, $\dot{y}(t)$ and $\ddot{y}(t)$ respectively denotes the first-order derivative and second-order derivative with respect to time t.

II. SYSTEM MODEL AND PROBLEM FORMULATION

A. SYSTEM MODEL

As shown in Fig. 1, a multi-UAV enabled wireless communication system is considered, where $M > 1$ UAVs are dispatched to collect information from $K > 1$ GTs that are randomly located at fixed positions. Let $\mathcal{M} = \{1, 2, ..., M\}$ and $\mathcal{K} = \{1, 2, ..., K\}$ denote the set of UAVs and GTs, respectively, with $|\mathcal{M}| = M$ and $|\mathcal{K}| = K$. Without loss of generality, a three-dimensional (3D) Cartesian coordinate system is considered. Hence, the location of each GT $k \in \mathcal{K}$ can be denoted as $\{\mathbf{w} = [x_k, y_k]^T\}_{k\in\mathcal{K}}$, $\mathbf{w} \in \mathbb{R}^{2\times 1}$. A finite period $T > 0$ is set to UAVs for mission completion. It is also assumed that these UAVs are equipped with the same bandwidth B for communication. During the period, these UAVs are assumed to fly at a fixed altitude H that corresponds to the minimum altitude to avoid collision with obstacles. As a result, at any time instant t, with $0 \le t \le T$, denote by $\mathbf{q}_m[n] = [x_m(t), y_m(t)]^T$ the time-varying trajectory coordinate projected on the horizontal plane. Besides, at any time instant, these UAVs are subject to the maximum/minimum speed and acceleration constraints, i.e., $\|\mathbf{v}_m(t)\| = \|\dot{\mathbf{q}}_m(t)\| \le V_{\max}$, $\|\mathbf{v}_m(t)\| \ge V_{\min}$ and $\|\mathbf{a}_m(t)\| = \|\ddot{\mathbf{q}}_m(t)\| \le a_{\max}$.

For serving GTs periodically, each UAV is assumed to fly return to launch point (RTL) at the end of period T, namely $\mathbf{q}_m(0) = \mathbf{q}_m(T)$, with $m \in \mathcal{M}$. Note that, for ensuring collision avoidance, a secure flight mechanism is proposed, in which any two UAVs need to keep a secure distance at any time instant, i.e., $\|\mathbf{q}_m(t) - \mathbf{q}_l(t)\|^2 \ge D^2, m, l \in \mathcal{M}, m \ne l$, where D refers to the minimum-security distance between UAVs.

For convenience, the discrete linear state-space approximation technique is applied in our design. The period T is discretized into N equally spaced time slots with an equal step size δ_t, with $\delta_t \ll T$, indexed by $n = 1, 2, ..., N$. Let $\mathcal{N} = \{1, 2, ..., N\}$ denote the time slot set, where $|\mathcal{N}| = N$. Based on this discretization method, the projected trajectory of the UAV m can be approximately characterized by a sequence $\{\mathbf{q}_m[n] = [x_m[n], y_m[n]]^T, \forall n \in \mathcal{N}, m \in \mathcal{M}\}$. As a result, all constraints discussed above can be equivalently expressed in discretization forms as

$$\mathbf{v}_m[n+1] = \mathbf{v}_m[n] + \mathbf{a}_m[n]\delta_t, \quad \forall m, \quad n = 1, 2, ..., N-1, \tag{1}$$

$$\mathbf{q}_m[n+1] = \mathbf{q}_m[n] + \mathbf{v}_m[n]\delta_t + \frac{1}{2}\mathbf{a}_m[n]\delta_t^2, \quad \forall m, \quad n = 1, 2, ..., N-1, \tag{2}$$

$$\|\mathbf{v}_m[n]\| \le V_{\max}, \quad \forall m, n, \tag{3}$$

$$\|\mathbf{v}_m[n]\| \ge V_{\min}, \quad \forall m, n, \tag{4}$$

$$\|\mathbf{a}_m[n]\| \le a_{\max}, \quad \forall m, n, \tag{5}$$

$$\mathbf{q}_m[1] = \mathbf{q}_m[N], \quad \forall m, \tag{6}$$

$$\|\mathbf{q}_m[n] - \mathbf{q}_l[n]\|^2 \ge D^2, \quad \forall m, l \in \mathcal{M}, \ m \ne l, n. \tag{7}$$

Where the constraints in (1) and (2) are respectively obtained based on first- and second-order Taylor approximation of the speed $\mathbf{v}_m[n]$ and trajectory $\mathbf{q}_m[n]$ [16]. Constraint in (7) is the proposed secure flight mechanism. Thus, the distance between UAV m and GT k in time slot $n \in \mathcal{N}$ can be expressed as

$$d_{m,k}[n] = \sqrt{\|\mathbf{q}_m[n] - \mathbf{w}_k\|^2 + H^2}. \tag{8}$$

For simplicity, the communication link between UAVs and GTs is assumed to be dominated by the LoS channel. Furthermore, the Doppler effect due to the UAVs' mobility is also assumed to be perfectly compensated at the receivers [20], [21], [25], [26]. Thus, the time-varying channel gain from GT k to UAV m within slot n follows the free-space path loss model, which can be expressed as

$$h_{m,k}[n] = \beta_0 d_{m,k}^{-2}[n] = \frac{\beta_0}{\|\mathbf{q}_m[n] - \mathbf{w}_k\|^2 + H^2}, \tag{9}$$

Where β_0 denotes the channel power at the reference distance $d_0 = 1$ meter. For interference avoidance, the multiple UAVs take turns to collect information from GTs over the orthogonal time slots. As thus, a binary variable $\alpha_{m,k}[n]$ is used to represent the communication scheduling that determines the optimal UAV-GT communication pair in slot n. The equality $\alpha_{m,k}[n] = 1$ indicates that UAV m collects information from GT k in slot n. Otherwise, let $\alpha_{m,k}[n] = 0$. Note that at any slot only one UAV-GT pair at most can be connected, which results in the following constraints

$$\sum_{m=1}^{M}\sum_{k=1}^{K}\alpha_{m,k}[n] \le 1, \quad \forall n, \tag{10}$$

$$\alpha_{m,k}[n] \in \{0, 1\}, \quad \forall m, k, n. \tag{11}$$

For simplicity, the energy supporting flight of per UAV is assumed to be sufficient during the serving time. Let $p_k[n]$ represent the uplink transmit power of GT k in slot n. Under our assumption, each GT has a maximum instantaneous power constraint $P_{\max} > 0$ in per slot, and its energy consumption for information transmission is subject to the total amount of energy $W > 0$ in joule, which yields the following constraints

$$\delta_t \sum_{n=1}^{N} p_k[n] \le W, \tag{12}$$

$$0 \le p_k[n] \le P_{\max}, \quad \forall k. \tag{13}$$

Initially, per GT stores the same amount of energy for information transmission. Based on the discussion above, the achievable rate in bits/second/Hz (bps/Hz) from GT K to UAV m within slot n can be obtained as

$$\begin{aligned} r_{m,k}[n] &= \alpha_{m,k}[n] \log_2(1 + \frac{h_{m,k}[n]p_k[n]}{\sigma^2}) \\ &= \alpha_{m,k}[n] \log_2(1 + \frac{\gamma_0 p_k[n]}{\|\mathbf{q}_m[n] - \mathbf{w}_k\|^2 + H^2}), \end{aligned} \tag{14}$$

Where σ^2 is the white Gaussian noise power at the UAV receiver, and $\gamma_0 = \beta_0/\sigma^2$ denotes the reference received signal-to-noise ratio (SNR) at $d_0 = 1$ meter. Thus, the throughput of GT k in bits/Hz during the period can be obtained as below

$$C_k = \delta_t \sum_{m=1}^{M} \sum_{n=1}^{N} r_{m,k}[n], \quad \forall k. \tag{15}$$

With (14), the throughput of UAV m over total N slots can be expressed as

$$\begin{aligned} C_m &= \delta_t \sum_{k=1}^{K} \sum_{n=1}^{N} r_{m,k}[n] \\ &= \delta_t \sum_{k=1}^{K} \sum_{n=1}^{N} \alpha_{m,k}[n] \log_2(1 + \frac{\gamma_0 p_k[n]}{\|\mathbf{q}_m[n] - \mathbf{w}_k\|^2 + H^2}), \end{aligned} \tag{16}$$

Accordingly, the system throughput over the period can be expressed as

$$\begin{aligned} C &= \sum_{m=1}^{M} C_m \\ &= \delta_t \sum_{m=1}^{M} \sum_{k=1}^{K} \sum_{n=1}^{N} \alpha_{m,k}[n] \log_2(1 + \frac{\gamma_0 p_k[n]}{\|\mathbf{q}_m[n] - \mathbf{w}_k\|^2 + H^2}). \end{aligned} \tag{17}$$

Here, a difference mechanism for the multi-UAV communication system is taken into account. Specifically, a weight factor θ_m is introduced, with $\theta_m \in [0, 1]$, to denote the throughput ratio for UAV m, which is defined as the required throughput of UAV m over the achievable throughput of the system. In practice, the fairness factor can be determined by the difference consideration between UAVs, such as UAV types, SWAP constraints, as well as communication performance. In addition, it also can be adjusted to satisfy the fair communication for multiple UAVs if there is fairness requirement in the system. Note that the factor is described as fairness/difference factor in the following sections. Evidently, the factor θ_m satisfies the constraint of $\sum_{m=1}^{M} \theta_m \le 1$. By given this, each UAV can be individually designed with difference consideration by flexibly adjusting the fairness factor. As a result, this new constraint can be concretely expressed as

$$C_m \ge \theta_m C, \quad \forall m. \tag{18}$$

In the proposed system, our objective is to maximize the minimum throughput of GTs in uplink channel. For ease of discussion, the optimization variables are represented by three blocks, i.e., $\mathbf{A} = \{\alpha_{m,k}[n], \forall m, k, n\}$, $\mathbf{P} = \{p_k[n], \forall k, n\}$, and $\mathbf{Q} = \{\mathbf{q}_m[n], \mathbf{v}_m[n], \mathbf{a}_m[n], \forall m, n\}$, which correspond to the communication scheduling , power allocation and flight plan design, respectively. In the proposed design, our goal is to maximize the minimum GT throughput. For ease of exposition, the minimum throughput of GTs can be expressed as

$$s = \min_{\forall k \in \mathcal{K}} C_k. \tag{19}$$

B. PROBLEM FORMULATION

Based on above discussion, the optimization problem is formulated as

$$\begin{aligned} \text{(P1):} \quad & \max_{s,\mathbf{A},\mathbf{P},\mathbf{Q}} \ s \\ & \text{s.t. } C_k \ge s, \forall k, \\ & \quad (1)\text{-}(7), (10)\text{-}(13) \text{ and } (18). \end{aligned} \tag{20}$$

It is worth highlighting that the constraint in (18) shows the difference design for multi-UAV, the constraints in (10) and (11) represent the communication scheduling. The constraint in (7) indicates the secure flight mechanism for collision avoidance between any two UAVs. Besides, both (12) and (13) affect the power allocation of GTs, and the constraints in (2)-(5) are kinetic limitations related to UAVs.

Note that problem (P1) is challenging to be solved optimally due to it is not a standard convex optimization problem. First, the left-hand sides (LHS) of the constraints in (20) is jointly non-concave with respect to $\mathbf{A}$, $\mathbf{P}$ and $\mathbf{Q}$. In addition, both sides of the constraint in (18) are non-convex with respect to $\mathbf{A}$, $\mathbf{P}$ and $\mathbf{Q}$. Second, the optimization variables $\mathbf{A}$ involve integer constraints due to the variables $\mathbf{A}$ are binary, as shown in (11). Consequently, problem (P1) is a mixed-integer non-convex optimization problem that can not be directly solved by using standard convex optimization techniques. In the next section, a feasible scheme is proposed to efficiently handle this problem.

III. PROPOSED SULOTION

To tackle problem (P1), an iterative technique is proposed in this section. Without loss of generality, the problem (P1) is decomposed into two subproblems. First, the communication

scheduling $\mathbf{A}$ and power allocation $\mathbf{P}$ are optimized for a given fixed trajectory $\mathbf{Q}^r$ (r denotes the r-th iteration), which is denoted by subproblem 1. By solving subproblem 1, the optimized communication scheduling and power allocation can be obtained, denoted by $\mathbf{A}^{r+1}$ and $\mathbf{P}^{r+1}$, respectively. Second, the trajectory $\mathbf{Q}$ is optimized for a fixed GT scheduling and power allocation (namely $\mathbf{A}^{r+1}$ and $\mathbf{P}^{r+1}$), which is denoted by subproblem 2. Thus, a suboptimal solution can be obtained by solving these two subproblems in an alternative iteration method.

A. SUBPROBLEM 1: OPTIMIZING COMMUNICATION SCHEDULING AND POWER ALLOCATION UNDER GIVEN FIXED TRAJECTORY

Under given fixed trajectory $\mathbf{Q}^r$, subproblem 1 can be expressed as

$$\text{(P1.1)}: \max_{s,\mathbf{A},\mathbf{P}} s \quad \text{s.t. (10)-(13), (18) and (20),}$$

Note that subproblem (P1.1) is still a non-convex and mixed-integer problem, because the communication scheduling $\mathbf{A}$ and power allocation $\mathbf{P}$ are still coupled in (18) and (20). In addition, the constraints in (10) and (11) involve integer constraints. To tackle these problems, the binary variable $\mathbf{A}$ for communication scheduling is relaxed into a set of continuous variables, i.e., $0 \le \alpha_{m,k}[n] \le 1, \forall m, k, n$. Then, slack variables $\{\tau_{m,k}[n]\}$ are introduced. Hence, problem (P1.1) can be reformulated as

$$\text{(P1.1.1)}: \max_{s,\mathbf{A},\mathbf{P},\{\tau_{m,k}[n]\}} s$$

$$\text{s.t. } \delta_t \sum_{m=1}^{M}\sum_{n=1}^{N} \alpha_{m,k}[n]\tau_{m,k}[n] \ge s, \quad \forall k, \tag{21a}$$

$$\delta_t \sum_{k=1}^{K}\sum_{n=1}^{N} \alpha_{m,k}[n]\tau_{m,k}[n] \ge \theta_m C, \quad \forall m, \tag{21b}$$

$$\log_2\Big(1+\frac{\gamma_0 p_k[n]}{\|\mathbf{q}_m^r[n]-\mathbf{w}_k\|^2+H^2}\Big) \ge \tau_{m,k}[n], \quad \forall m,k,n, \tag{21c}$$

$$\sum_{m=1}^{M}\sum_{k=1}^{K} \alpha_{m,k}[n] \le 1, \quad \forall n, \tag{21d}$$

$$0 \le \alpha_{m,k}[n] \le 1, \quad \forall m,k,n. \tag{21e}$$

It can be verified that the optimal solution of problem (P1.1.1) satisfies the constraint in (21c) with equality, since otherwise $\tau_{m,k}[n]$ can be appropriately increased to achieve a higher upper boundary of the objective value of s in (21a). As a result, the objective value would increase. Also, the constraint (21d) must be met with equality in the optimal solution to problem (P1.1.1), we can easily reconstruct a binary solution by further dividing each time slot into sub-slots until the binary solution brings zero relaxation gap. This procedure is described in detail in [20].

Note that the constraints in (21c)-(21e) are convex, whereas the LHS of (21a) and (21b) are still non-concave due to the variables $\mathbf{A}$ and slack variables $\{\tau_{m,k}[n]\}$ being coupled. To deal with this problem, a local convex approximation method that can be guaranteed to converge to a locally optimal solution is applied. Specifically, the LHS of the constraint in (21a) can be expressed as below

$$\alpha_{m,k}[n]\tau_{m,k}[n] = \frac{(\alpha_{m,k}[n]+\tau_{m,k}[n])^2}{2} - \frac{\alpha_{m,k}^2[n]+\tau_{m,k}^2[n]}{2}, \tag{22}$$

Then, the local convex approximation method is applied to deal with the first term of the right-hand side (RHS) of the constraint in (22). For the RHS of the constraint in (22), the first term of the numerator is jointly convex with respect to $\alpha_{m,k}[n]$ and $\tau_{m,k}[n]$. Thus, its first-order Taylor expansion is the global under-estimator [27]. As a result, for any local point $\{\alpha_{m,k}^r[n], \tau_{m,k}^r[n]\}$, a lower bound function can be defined as below

$$\begin{aligned}&(\alpha_{m,k}[n]+\tau_{m,k}[n])^2\\ &\ge (\alpha_{m,k}^r[n]+\tau_{m,k}^r[n])^2\\ &\quad +2(\alpha_{m,k}^r[n]+\tau_{m,k}^r[n])(\alpha_{m,k}[n]-\alpha_{m,k}^r[n])\\ &\quad +2(\alpha_{m,k}^r[n]+\tau_{m,k}^r[n])(\tau_{m,k}[n]-\tau_{m,k}^r[n]) \triangleq \rho_{m,k}^{lb}[n].\end{aligned} \tag{23}$$

It is worth noting that both sides of the inequality in (21b) are non-convex, which means that the RHS of (21b) as well needs to be appropriately tackled. To this end, a relaxation variable s_2 is introduced to rewrite (21b) as

$$\delta_t \sum_{k=1}^{K}\sum_{n=1}^{N} \alpha_{m,k}[n]\tau_{m,k}[n] \ge \theta_m s_2, \quad \forall m, \tag{24}$$

Where

$$s_2 \le \delta_t \sum_{m=1}^{M}\sum_{k=1}^{K}\sum_{n=1}^{N} \alpha_{m,k}[n]\log_2\Big(1+\frac{\gamma_0 p_k[n]}{\|\mathbf{q}_m^r[n]-\mathbf{w}_k\|^2+H^2}\Big), \tag{25}$$

$$s_2 \ge K \cdot s, \tag{26}$$

In fact, by introducing the relaxation variable s_2, the system throughput C is relaxed into a restricted range as shown in (25) and (26). It can be verified that the optimal solution of problem (P1.1.1) must satisfy the constraints in (25) and (26) with equality, since otherwise the value of s_2 in (25) can always be appropriately increased without decreasing the objective value of s. So, the objective value in (26) can constantly increase until the equality holds. As a result, with (22)-(26), an equivalent transformation of problem (P1.1.1) can be obtained as below

$$\text{(P1.1.2)}: \max_{s,\mathbf{A},\mathbf{P},\{\tau_{m,k}[n]\},s_2} s$$

$$\text{s.t. } \delta_t \sum_{m=1}^{M}\sum_{n=1}^{N} \frac{\rho_{m,k}^{lb}[n]-(\alpha_{m,k}^2[n]+\tau_{m,k}^2[n])}{2} \ge s, \quad \forall k, \tag{27a}$$

$$\delta_t \sum_{k=1}^{K}\sum_{n=1}^{N} \frac{\rho_{m,k}^{lb}[n]-(\alpha_{m,k}^2[n]+\tau_{m,k}^2[n])}{2} \geq \theta_m s_2, \quad \forall m, \tag{27b}$$

$$\delta_t \sum_{m=1}^{M}\sum_{k=1}^{K}\sum_{n=1}^{N} \frac{\rho_{m,k}^{lb}[n]-(\alpha_{m,k}^2[n]+\tau_{m,k}^2[n])}{2} \geq s_2 \tag{27c}$$

$$s_2 \geq K \cdot s, \tag{27d}$$

$$\log_2(1+\frac{\gamma_0 p_k[n]}{\|\mathbf{q}_m^r[n]-\mathbf{w}_k\|^2+H^2}) \geq \tau_{m,k}[n], \quad \forall m,k,n, \tag{27e}$$

$$\sum_{m=1}^{M}\sum_{k=1}^{K}\alpha_{m,k}[n] \leq 1, \quad \forall n, \tag{27f}$$

$$0 \leq \alpha_{m,k}[n] \leq 1, \quad \forall m,k,n. \tag{27g}$$

Note that (P1.1.2) is a convex problem, which can be solved effectively by standard convex tools. By solving problem (P1.1.2), the optimized communication scheduling and power allocation are obtained. Then, both would be served as the inputs for problem (P1.2) in the next subsection.

B. SUBPROBLEM 2: OPTIMIZING THE TRAJECTORY UNDER GIVEN FIXED COMMUNICATION SCHEDULING AND POWER ALLOCATION

In this subsection, the flight plan design problem can be optimized for given fixed local points of communication scheduling and power allocation, denoted as $\{\mathbf{A}^{r+1}, \mathbf{P}^{r+1}\}$. Thus, subproblem 2 can be obtained as

$$\text{(P1.2)}: \max_{s,\mathbf{Q}} s$$
$$\text{(1)-(7), (18) and (20),}$$

Problem (P1.2) is also a non-convex problem due to the non-convex constraints in (18), (20), (4) and (7). Note that the constraint in (2) is convex as it is linear with respect to $\mathbf{q}[n]$, $\mathbf{v}[n]$ and $\mathbf{a}[n]$. Similarly, the constraint in (1) is also convex. To deal with these non-convex constraints in problem (P1.2), the inequality in (20) is rewritten as

$$\delta_t \sum_{m=1}^{M}\sum_{n=1}^{N}\alpha_{m,k}^{r+1}[n]\log_2(1+\frac{\gamma_0 p_k^{r+1}[n]}{\|\mathbf{q}_m[n]-\mathbf{w}_k\|^2+H^2}) \geq s, \tag{28}$$

It is worth noting that the LHS of the inequality (28) can be converted into a convex expression if considering $\|\mathbf{q}_m[n]-\mathbf{w}_k\|^2$ as a whole. Thus, by applying sequential convex optimization technique at any given points $\{\mathbf{q}_m^r[n]-\mathbf{w}_k\}$, the LHS of the inequality in (28) can be lower-bounded by

$$\begin{aligned}
&\delta_t \sum_{m=1}^{M}\sum_{n=1}^{N}\alpha_{m,k}^{r+1}[n]\log_2(1+\frac{\gamma_0 p_k^{r+1}[n]}{\|\mathbf{q}_m[n]-\mathbf{w}_k\|^2+H^2}) \\
&\geq \delta_t \sum_{m=1}^{M}\sum_{n=1}^{N}[\varphi_{m,k}^{r+1}[n]-\psi_{m,k}^{r+1}[n](\|\mathbf{q}_m[n]-\mathbf{w}_k\|^2 \\
&\quad -\|\mathbf{q}_m^r[n]-\mathbf{w}_k\|^2)] \\
&\triangleq C_{k,lb}^{r+1},
\end{aligned} \tag{29}$$

Where

$$\begin{aligned}
&\varphi_{m,k}^{r+1}[n] \\
&= \alpha_{m,k}^{r+1}[n]\log_2(1+\frac{\gamma_0 p_k^{r+1}[n]}{\|\mathbf{q}_m^r[n]-\mathbf{w}_k\|^2+H^2}),
\end{aligned} \tag{30}$$

$$\begin{aligned}
&\psi_{m,k}^{r+1}[n] \\
&= \frac{\log_2(e)\alpha_{m,k}^{r+1}[n]\gamma_0 p_k^{r+1}[n]}{(\|\mathbf{q}_m^r[n]-\mathbf{w}_k\|^2+H^2)(\|\mathbf{q}_m^r[n]-\mathbf{w}_k\|^2+H^2+\gamma_0 p_k^{r+1}[n])}
\end{aligned} \tag{31}$$

For the sake of easy discussion, define

$$\xi_{m,k}^{r+1} \triangleq \varphi_{m,k}^{r+1}[n]-\psi_{m,k}^{r+1}[n](\|\mathbf{q}_m[n]-\mathbf{w}_k\|^2-\|\mathbf{q}_m^r[n]-\mathbf{w}_k\|^2). \tag{32}$$

To solve the non-convex constraint in (18), the same technique as tackling the constraint in (21b) of problem (P1.1) is applied. By introducing a slack variable $\check{s}_2$, the constraint in (18) can be expressed as

$$\begin{aligned}
C_m &= \delta_t \sum_{k=1}^{K}\sum_{n=1}^{N} r_{m,k}[n] \\
&= \delta_t \sum_{k=1}^{K}\sum_{n=1}^{N}\alpha_{m,k}^{r+1}[n]\log_2(1+\frac{\gamma_0 p_k^{r+1}[n]}{\|\mathbf{q}_m[n]-\mathbf{w}_k\|^2+H^2}) \\
&\geq \theta_m \check{s}_2,
\end{aligned} \tag{33}$$

Where

$$\check{s}_2 \leq \delta_t \sum_{m=1}^{M}\sum_{k=1}^{K}\sum_{n=1}^{N}\alpha_{m,k}^{r+1}[n]\log_2(1+\frac{\gamma_0 p_k^{r+1}[n]}{\|\mathbf{q}_m[n]-\mathbf{w}_k\|^2+H^2}), \tag{34}$$

$$\check{s}_2 \geq K \cdot s, \tag{35}$$

Similarly, the optimal solution of problem (P1.2) also satisfies the constraints in (34) and (35) with equality. As for the LHS of the inequality constraint in (33) and the RHS of the constraint in (34), their lower bound functions can be respectively obtained by applying the first-order Taylor expansion at given point $\{\mathbf{q}_m^r[n]-\mathbf{w}_k\}$ as follows

$$C_{m,lb}^{r+1} \triangleq \delta_t \sum_{k=1}^{K}\sum_{n=1}^{N}\xi_{m,k}^{r+1}[n], \tag{36}$$

$$C_{lb}^{r+1} \triangleq \delta_t \sum_{m=1}^{M}\sum_{k=1}^{K}\sum_{n=1}^{N}\xi_{m,k}^{r+1}[n], \tag{37}$$

Where $\xi_{m,k}^{r+1}[n]$ is subjected to the equality in (32). Next, rewrite the non-convex constraint in (4) as follows

$$\|\mathbf{v}_m[n]\|^2 \geq V_{\min}^2, \quad \forall m,n, \tag{38}$$

Consider the constraint in (38) is still a non-convex expression, the local convex approximation technique can be applied to tackle the LHS of the constraint, since $\|\mathbf{v}_m[n]\|^2$ is convex and differentiable with respect to $\mathbf{v}_m[n]$. As a result, its lower-bound function is obtained based on the fact that the

global under-estimator of a convex differentiable function can be obtained by its first-order Taylor expansion [27]. Thus, for any given point $\{\mathbf{v}_m^r[n]\}$, the LHS of the constraint in (38) can be lower-bounded as

$$\begin{aligned}\|\mathbf{v}_m[n]\|^2 &\geq \|\mathbf{v}_m^r[n]\|^2 + 2(\mathbf{v}_m^r[n])^T(\mathbf{v}_m[n]-\mathbf{v}_m^r[n]) \\ &\triangleq \chi_{lb,m}[n], \quad \forall m, n. \end{aligned} \tag{39}$$

Hence define a new constraint,

$$\chi_{lb,m}[n] \geq V_{\min}^2, \quad \forall m, n. \tag{40}$$

Note that the non-convex constraint in (7) also needs to be tackled. Specifically, auxiliary variables $\{\mathbf{x}_{m,l}[n]\}$ are introduced, and let

$$\|\mathbf{x}_{m,l}[n]\|^2 \geq D^2, \tag{41}$$

Where

$$\mathbf{x}_{m,l}[n] = \mathbf{q}_m[n] - \mathbf{q}_l[n], \quad \forall n \in \mathcal{N}, m, l \in \mathcal{M}, \ m \neq l. \tag{42}$$

With such a reformulation, the constraint in (7) is partitioned into two parts as shown in (41) and (42). The equality in (42) is a linear constraint, whereas the inequality in (41) is still a non-convex expression. To tackle (41), the same technique as used in (38) is applied. Therefore, a lower-bound function at given points $\{\mathbf{x}_{m,l}^r[n]\}$ is obtained as below

$$\begin{aligned}\xi_{m,l,lb}[n] &\triangleq \|\mathbf{x}_{m,l}^r[n]\|^2 + 2(\mathbf{x}_{m,l}^r[n])^T(\mathbf{x}_{m,l}[n]-\mathbf{x}_{m,l}^r[n]) \\ &\geq D^2, \quad \forall m, l, \ m \neq l, n, \end{aligned} \tag{43}$$

In fact, the given points $\{\mathbf{x}_{m,l}^r[n]\}$ can be set as $\mathbf{x}_{m,l}^r[n] = \mathbf{q}_m^r[n] - \mathbf{q}_l^r[n]$ at the r-th iteration due to the equality always holding in (42).

All the non-convex constraints of problem (P1.2) have now been analyzed and appropriately tackled, and the problem (P1.2) can be reformulated as

(P1.2.1):

$$\max_{s,\mathbf{Q},\check{s}_2,\{\mathbf{x}_{m,l}[n]\}} \quad s$$

s.t. (1)-(3), (5), (6)

$$C_{k,lb}^{r+1} \geq s, \quad \forall k, \tag{44a}$$

$$C_{m,lb}^{r+1} \geq \theta_m \check{s}_2, \quad \forall m, \tag{44b}$$

$$C_{lb}^{r+1} \geq \check{s}_2, \quad \forall m, \tag{44c}$$

$$\check{s}_2 \geq K \cdot s, \tag{44d}$$

$$\chi_{lb,m}[n] \geq V_{\min}^2, \quad \forall m, n, \tag{44e}$$

$$\xi_{m,l,lb}[n] \geq D^2, \quad \forall m, l, \ m \neq l, n, \tag{44f}$$

$$\mathbf{x}_{m,l}[n] = \mathbf{q}_m[n] - \mathbf{q}_l[n], \quad \forall m, l, \ m \neq l, n. \tag{44g}$$

Based on the previous discussions, problem (P1.2.1) is distinctly equivalent to problem (P1.2), and problem (P1.2.1) is a convex problem that can be directly and effectively solved by convex optimization tools such as CVX [28].

C. PROPOSED ALGORITHM

In this subsection, an iterative algorithm is proposed for solving problem (P1). From the previous discussion, problem (P1) can be equivalently solved by alternately optimizing subproblem (P1.1.2) and (P1.2.1). By this, a suboptimal solution can be obtained. To summarize, the iterative algorithm to solve problem (P1) is proposed as shown in Algorithm 1.

Algorithm 1 Iterative Algorithm for Problem (P1)

1: Initialize $\{\mathbf{A}^r, \mathbf{P}^r, \mathbf{Q}^r\}$, variables $\{\tau_{m,k}^r[n], \mathbf{x}_{m,l}^r[n]\}$ and let iteration index $r = 0$, tolerance $\varepsilon > 0$.
2: **repeat**
3: Solve problem (P1.1.2) for given $\{\mathbf{Q}^r, \tau_{m,k}^r[n]\}$, and denote the optimized solution as $\{\mathbf{A}^r, \mathbf{P}^r, \tau_{m,k}^r[n]\}^*$.
4: Set $\{\mathbf{A}^{r+1}, \mathbf{P}^{r+1}, \tau_{m,k}^{r+1}[n]\} \leftarrow \{\mathbf{A}^r, \mathbf{P}^r, \tau_{m,k}^r[n]\}^*$.
5: Solve problem (P1.2.1) for given $\{\mathbf{A}^{r+1}, \mathbf{P}^{r+1}, \mathbf{Q}^r, \mathbf{x}_{m,l}^r[n]\}$, and denote the optimized solution as $\{\mathbf{Q}^r, \mathbf{x}_{m,l}^r[n]\}^*$.
6: Set $\{\mathbf{Q}^{r+1}, \mathbf{x}_{m,l}^{r+1}[n]\} \leftarrow \{\mathbf{Q}^r, \mathbf{x}_{m,l}^r[n]\}^*$.
7: Set $r \leftarrow r + 1$.
8: **until** The objective value converges to the prescribed accuracy ε.

D. TRAJECTORY INITIALIZATION

In this subsection, a simple and effective trajectory initialization method for Algorithm 1 is represented. It is critical for Algorithm 1 to determine a feasible initial trajectory, since the constraints in (2)-(6) are complex and not easy to be satisfied. To seek a feasible initial method, a simple circular path scheme is proposed. Theoretically, under the premise of satisfying the constraints in (2)-(6), the circular trajectories that correspond to different UAVs can be set at any positions within the goal area. Specifically, the circle centers of different trajectories are set at different points near the geometrical center of the goal area. Thus, the center of each UAV's trajectory can be denoted by $\mathbf{O}_m = [x_m, y_m]^T$. To better balance the GTs' rate, each UAV's speed is set as a constant and reasonable value V, with $V_{\min} \leq V \leq V_{\max}$. Thus, each UAV has the same radius denoted by $r = \frac{VT}{2\pi}$. Thereby, for $n \in \mathcal{N}$, the initial trajectory of UAV m can be denoted as

$$\mathbf{q}_m^0[n] = [x_m + r\sin\frac{2\pi(n-1)}{N-1}, y_m + r\cos\frac{2\pi(n-1)}{N-1}]^T. \tag{45}$$

IV. NUMERICAL RESULTS

In this section, numerical results are provided to demonstrate the validity of the proposed algorithm. A vector $\boldsymbol{\theta} \in \mathbb{R}^{1\times M}$ is used to present the value of fairness factor for multiple UAVs, i.e., $\theta_m \in \boldsymbol{\theta}$ denotes the fairness factor of the m-th UAV. All GTs in the system are assumed to be randomly distributed in a 2D rectangular area of 2×2 km^2 as shown in Fig. 2, marked by '☆'s. As shown in Fig. 2, Fig. 3 as well as Fig. 4,

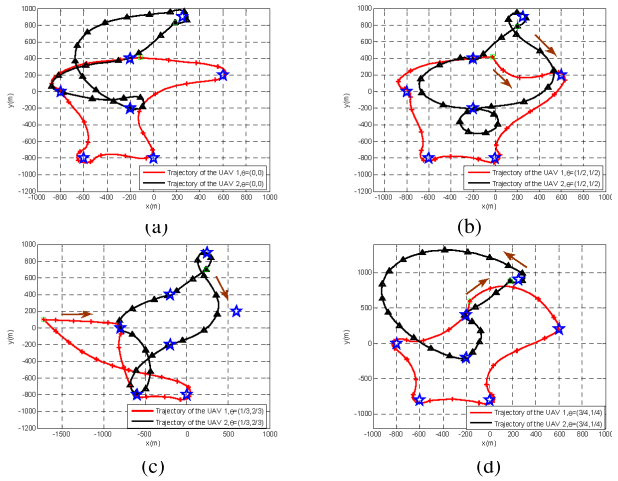

FIGURE 2. Comparison of the optimal trajectories of two UAVs under different fairness factors for $T = 150$ s.

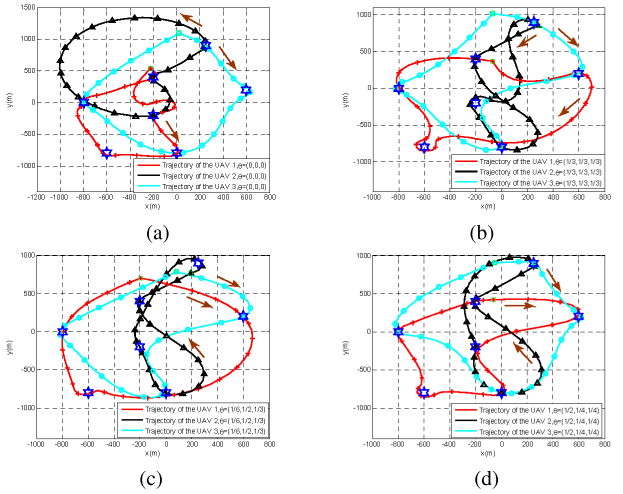

FIGURE 3. Comparison of the optimal trajectories of three UAVs under different fairness factors for $T = 150$ s.

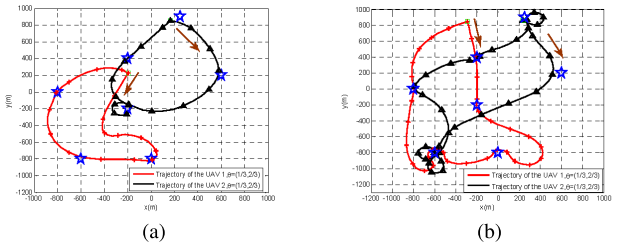

FIGURE 4. Comparison of the optimal trajectories of two UAVs with the fairness factors $\theta = (1/3, 2/3)$ for different periods. (a) $T = 100$ s. (b) $T = 200$ s.

the original/final positions of UAVs are marked by '□'s. To illustrate each UAV position in per slot, the trajectories are sampled every 6 seconds, and the sampled points are marked by '+'s, '△'s or '◯'s. Specifically, all the rest of system parameters are set as shown in Table 2.

In Fig. 2, two UAVs' trajectories are illustrated under different fairness factors for period $T = 150$ s. Note that $\boldsymbol{\theta} = \mathbf{0}$ represents no difference to be considered. It can be observed

TABLE 2. System parameters for numerical simulation.

Symbolic Meaning	Symbol and Value
Altitude of UAVs	$H = 100$ m
Amount of GTs	$K = 7$
Maximum speed	$V_{\max} = 50$ m/s
Minimum speed	$V_{\min} = 20$ m/s
Maximum acceleration	$a_{\max} = 5$ m/s^2
Minimum-security distance	$D = 10$ m
Time slot size	$\delta_t = 2$ s
Maximum instantaneous power of each GT	$P_{\max} = 0.5$ w
Total energy of each GT	$W = 5$ J
Noise power spectrum density	$N_0 = -170$ dBm/Hz
Noise power	$\sigma^2 = N_0 B = -110$ dBm
Reference channel power	$\beta_0 = -50$ dB
Accuracy	$\varepsilon = 10^{-3}$
Communication bandwidth	$B = 1$ MHz

from Fig. 2 that each UAV first accelerates to fly closer to its served GT for a better channel link, and then decelerates and even hovers over the GT for more information collection. In addition, the different fairness factors result in big changes of the trajectories, which indicates that the optimal UAVs' flight paths depend on the value of the predetermined fairness factor. Intuitively, the UAVs can maximally exploit the mobility to serve GTs with the best air-to-ground channels for $\boldsymbol{\theta} = (0, 0)$. As a result, in these cases of considering the difference between the UAVs (see, e.g. Fig. 2(b)-(d)), the mobility of UAVs is restricted to some extent so as to meet the different fairness factor constraints. Generally speaking, if the gap between the fairness factors for these two UAVs is larger, the compromise of one UAV on mobility would be more severe. To show the case of more than two UAVs, in Fig. 3, the trajectories of three UAVs are plotted for period $T = 150$ s. Similarly, we can observe that each UAV is compelled to adjust its trajectory to satisfy the different fairness factor requirement.

In order to further illustrate the trajectories under different periods T, the optimal trajectories of two UAVs for fairness factor $\boldsymbol{\theta} = (1/3, 2/3)$ under different periods is plotted, as shown in Fig. 4. From Fig. 2(c) and Fig. 4, it can be observed that the period impacts the path planning of UAVs as well. In general, with lager T , it provides more flexibility for UAVs' flight plan design.

The convergence performance of the proposed Algorithm 1 is shown in Fig. 5. In this picture, the max-min GT throughput in Megabits (Mb) at each iteration for $T = 150$ s is plotted. Specifically, multi-UAV cases with different fairness factors are compared in order to illustrate the effect of different difference consideration on the system throughput. It can be observed that the max-min GT throughput with the difference consideration is lower than the case without difference consideration, i.e., $\boldsymbol{\theta} = \mathbf{0}$. This is because the difference factor restricts the UAVs' mobility to some extent. Besides, it also can be observed that the case of three UAVs outperforms the case of two UAVs, because under the former case, the communication coverage ability is superior, and there is more likely to obtain a shorter link

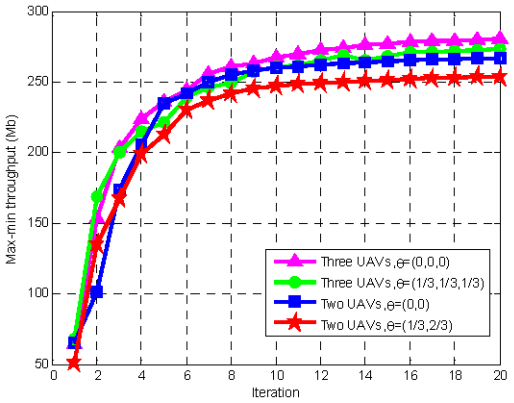

FIGURE 5. Convergence of the proposed Algorithm 1 for $T = 150$ s.

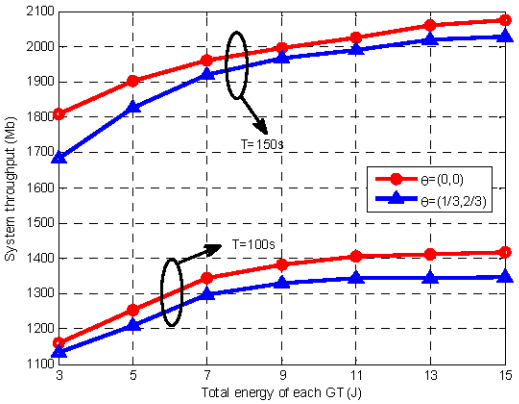

FIGURE 7. System throughput versus each GT's energy for period $T = 150$ s.

between the UAVs and GTs in each time slot so that leads to a larger throughput.

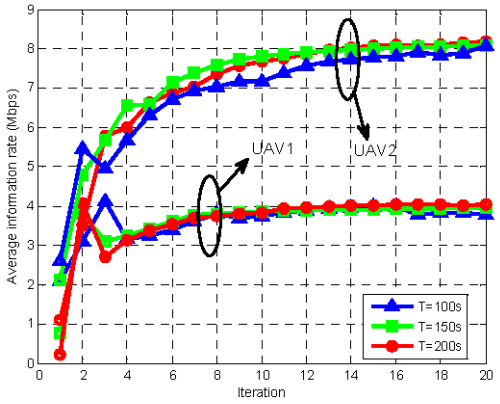

FIGURE 6. Average information rate of each UAV with fairness factor $\theta = (1/3, 2/3)$.

To further show the validity of the proposed Algorithm 1, the throughput of the case of two UAVs during different periods are illustrated in Fig. 6. For the sake of intuitive comparison, the average information rate of each UAV in Mbps with the fairness factor $\boldsymbol{\theta} = (1/3, 2/3)$ under different periods is shown in this picture. Note that the average information rate of each UAV can be readily obtained by the expression C_m/T, where C_m denotes the throughput of the UAV m as shown in (16). From Fig. 6, it first can be observed that the throughput of each UAV converges to a stable value under the required fairness factor constraint. The curves match our expectation and validate the proposed algorithm. Second, it can be also observed that one UAV's throughput increase may be at the expense of decreasing the other's in order to satisfy the fairness factor constraint. This indicates that the proposed Algorithm 1 is reliable, and the fairness factor indeed shows the difference design in the multi-UAV enabled system.

Fig. 7 shows the system throughput versus each GT's energy W for different period T and $\boldsymbol{\theta}$ under the case of two UAVs. It is observed that the system throughput rises rapidly when the total energy of each GT is low, then it raises smoothly with the increasing value of W. This is because each GT is subject to a maximum instantaneous transmit power in each slot as shown in (13). With the increasing value of W, the UAVs would gradually get into saturation states, in which the UAVs have less freedom to further improve the throughput via power allocation due to the constraint in (13). In Fig. 7, it also can be observed that for any period T, the case of $\boldsymbol{\theta} = (0, 0)$ always achieves the best system throughput. This is because the UAVs have the largest freedom for exploiting the mobility when there is no fairness factor limit.

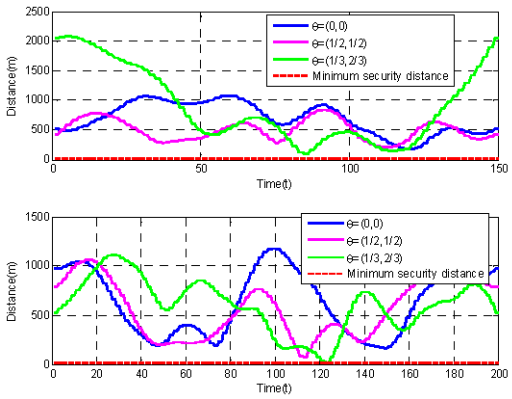

FIGURE 8. The distance between the two UAVs versus time for different period T.

Next, to show the effectiveness of the proposed flight security scheme, the distance between the UAVs in each slot for period $T = 150$ s and $T = 200$ s under different fairness factors are shown in Fig. 8. Without loss of generality, we show the case of two UAVs in Fig. 8. It can be observed that the trajectories follow the flight security scheme even though in many slots the distance between the UAVs is near even touches the minimum secure flight distance D (such as at $t = 123$ s for the case of $\boldsymbol{\theta} = (1/3, 2/3)$ for $T = 200$ s). Therefore, these observations in Fig. 8

demonstrate the effectiveness of the proposed flight security scheme.

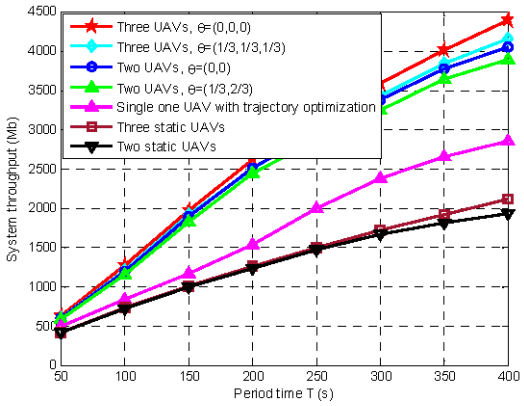

FIGURE 9. System throughput versus UAVs flight period T.

Fig. 9 shows the system throughput versus the different flight period T. Specially, the cases of two/three static UAVs and one single UAV are set as benchmarks. Note that in static UAV cases, the UAVs are assumed to stay stationary at fixed positions. While the case of single one UAV with flight plan design can be solved by Algorithm 1 by setting $M = 1$ and ignoring the difference consideration, i.e., the constraint in (18). In Fig. 9, it can be observed that for the proposed multi-UAV case, the system throughput grows much faster than that of the benchmarks. This indicates that the proposed multi-UAV design is far superior to the benchmarks mainly for two reasons. First, in our proposed design, the UAVs are able to exploit their mobility to fly closer to their serviced GTs and even hover over them to take advantage of the best channels. Second, a larger number of UAVs can improve the communication coverage ability and easily obtain shorter link between the UAVs and GTs in each time slot compared to the cases with fewer number of UAVs.

Nevertheless, it is worth noting that a larger period T or a larger number of UAVs does not imply a better performance when taking account of the system's cost, such as the UAVs' energy consumption. To illustrate this problem, the energy efficiency (EE) of UAVs in kbits/J obtained by $\frac{C}{M\bar{P}T}$ is shown in Fig. 10. Note that C denotes the system throughput as shown in (17), M and $\bar{P}$ denote the number of UAVs and average propulsion power for each UAV flight, respectively. Without loss of generality, the average propulsion power is set as $\bar{P} = 200$ w. From Fig. 10, it can be observed that the EE for multi-UAV cases does not increase with the number of UAVs. In addition, for each multi-UAV case, it illustrates that there is always an optimal period that leads to the maximum energy-efficient design, which means that the period time for task completion could be optimized while taking the system's cost into account. These give us new study freedom to seek a balance among multiple UAVs, system cost and period time, which will be left to our future work.

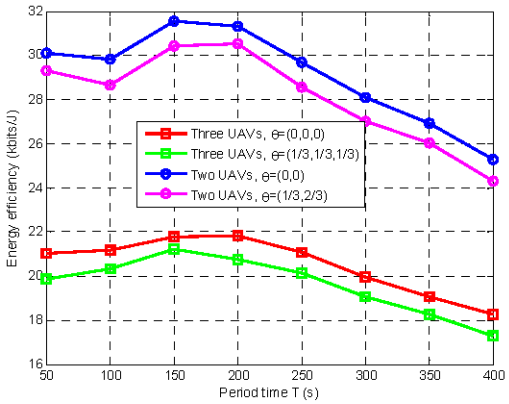

FIGURE 10. Energy efficiency versus UAVs flight period T.

V. CONCLUSION

A new multi-UAV enabled wireless communication system with difference consideration of UAVs is represented in this paper. Specifically, by taking account of the fairness/difference factor and secure flight requirement, this problem is formulated as a minimum GT throughput maximization problem that is a mixed integer non-convex problem. To solve this problem, an iterative algorithm that jointly optimizes the communication scheduling, power allocation and flight plan design is proposed. A suboptimal solution is obtained by applying the block coordinate descent, relaxation, and successive convex optimization techniques. Numerical results validate the effectiveness of our proposed design, and also show that the design achieves a significant performance gain compared to the benchmark. For multi-UAV enabled communication systems with difference consideration in future, the results achieved in this paper are expected to provide useful insights and guidelines for tackling similar problems.

ACKNOWLEDGEMENTS

The author declares that there is no conflict of interest regarding the publication of this paper.

REFERENCES

[1] Y. Zeng, R. Zhang, and T. J. Lim, "Wireless communications with unmanned aerial vehicles: Opportunities and challenges," *IEEE Commun. Mag.*, vol. 54, no. 5, pp. 36–42, May 2016.
[2] J. Valente, D. Sanz, A. Barrientos, J. del Cerro, Á. Ribeiro, and C. Rossi, "An air-ground wireless sensor network for crop monitoring," *Sensors*, vol. 11, no. 6, pp. 6088–6108, Jun. 2011.
[3] S. Waharte and N. Trigoni, "Supporting search and rescue operations with UAVs," in *Proc. IEEE Int. Conf. Emerg. Sec. Technol.*, Sep. 2010, pp. 142–147.
[4] P. Yang, X. Cao, C. Yin, Z. Xiao, X. Xi, and D. Wu, "Proactive drone-cell deployment: Overload relief for a cellular network under flash crowd traffic," *IEEE Trans. Intell. Transp. Syst.*, vol. 18, no. 10, pp. 2877–2892, Oct. 2017.
[5] S. Zhang, H. Zhang, Q. He, K. Bian, and L. Song, "Joint trajectory and power optimization for UAV relay networks," *IEEE Commun. Lett.*, vol. 22, no. 1, pp. 161–164, Jan. 2018.
[6] L. Xie, J. Xu, and R. Zhang. (Jan. 2018). "Throughput maximization for UAV-enabled wireless powered communication networks." [Online]. Available: http://arxiv.org/abs/1801.04545v2

[7] M. Mozaffari, W. Saad, M. Bennis, and M. Debbah, "Mobile Internet of Things: Can UAVs provide an energy-efficient mobile architecture?" in *Proc. IEEE Global Commun. Conf. (GLOBECOM)*, Washington, DC, USA, Dec. 2016, pp. 1–6.

[8] S. Hayat, E. Yanmaz, and R. Muzaffar, "Survey on unmanned aerial vehicle networks for civil applications: A communications viewpoint," *IEEE Commun. Surveys Tuts.*, vol. 18, no. 4, pp. 2624–2661, 4th Quart., 2016.

[9] H. Shakhatreh *et al.* (Apr. 2018). "Unmanned aerial vehicles: A survey on civil applications and key research challenges." [Online]. Available: https://arxiv.org/abs/1805.00881

[10] V. V. Chetlur and H. S. Dhillon, "Downlink coverage analysis for a finite 3-D wireless network of unmanned aerial vehicles," *IEEE Trans. Commun.*, vol. 65, no. 10, pp. 4543–4558, Jul. 2017.

[11] X. Zhang and L. Duan, "Optimization of emergency UAV deployment for providing wireless coverage," in *Proc. IEEE Global Commun. Conf. (GLOBECOM)*, Singapore, Dec. 2017, pp. 1–6.

[12] J. Lyu, Y. Zeng, R. Zhang, and T. J. Lim, "Placement optimization of UAV-mounted mobile base stations," *IEEE Commun. Lett.*, vol. 21, no. 3, pp. 604–607, Mar. 2017.

[13] R. I. Bor-Yaliniz, A. El-Keyi, and H. Yanikomeroglu, "Efficient 3-D placement of an aerial base station in next generation cellular networks," in *Proc. IEEE Int. Conf. Commun. (ICC)*, Kuala Lumpur, Malaysia, May 2016, pp. 1–5.

[14] M. Mozaffari, W. Saad, M. Bennis, and M. Debbah, "Efficient deployment of multiple unmanned aerial vehicles for optimal wireless coverage," *IEEE Commun. Lett.*, vol. 20, no. 8, pp. 1647–1650, Aug. 2016.

[15] V. Sharma, M. Bennis, and R. Kumar, "UAV-assisted heterogeneous networks for capacity enhancement," *IEEE Commun. Lett.*, vol. 20, no. 6, pp. 1207–1210, Jun. 2016.

[16] Y. Zeng and R. Zhang, "Energy-efficient UAV communication with trajectory optimization," *IEEE Trans. Wireless Commun.*, vol. 16, no. 6, pp. 3747–3760, Jun. 2017.

[17] H. Wang, G. Ding, F. Gao, J. Chen, J. Wang, and L. Wang. (Nov. 2017). "Power control in UAV-supported ultra dense networks: Communications, caching, and energy transfer." [Online]. Available: http://arxiv.org/abs/1712.05004

[18] K. Li, W. Ni, X. Wang, R. P. Liu, S. S. Kanhere, and S. Jha, "Energy-efficient cooperative relaying for unmanned aerial vehicles," *IEEE Trans. Mobile Comput.*, vol. 15, no. 9, pp. 1377–1386, Jun. 2016.

[19] M. Mozaffari, W. Saad, M. Bennis, and M. Debbah, "Unmanned aerial vehicle with underlaid device-to-device communications: Performance and tradeoffs," *IEEE Trans. Wireless Commun.*, vol. 15, no. 6, pp. 3949–3963, Jun. 2016.

[20] Q. Wu, Y. Zeng, and R. Zhang, "Joint trajectory and communication design for multi-UAV enabled wireless networks," *IEEE Trans. Wireless Commun.*, vol. 17, no. 3, pp. 2109–2121, Mar. 2018.

[21] Q. Wu and R. Zhang. (Jan. 2018). "Common throughput maximization in UAV-enabled OFDMA systems with delay consideration." [Online]. Available: https://arxiv.org/abs/1801.00444

[22] K. A. Ghamry, M. A. Kamel, and Y. Zhang, "Multiple UAVs in forest fire fighting mission using particle swarm optimization," in *Proc. Int. Conf. Unmanned Aircr. Syst.,* Miami, FL, USA, Jun. 2017, pp. 1404–1409.

[23] M. Horiuchi, H. Nishiyama, N. Kato, F. Ono, and R. Miura, "Throughput maximization for long-distance real-time data transmission over multiple UAVs," in *Proc. IEEE Int. Conf. Commun. (ICC)*, Kuala Lumpur, Malaysia, May 2016, pp. 1–6.

[24] Z. Guo, Z. Wei, Z. Feng, and N. Fan, "Coverage probability of multiple UAVs supported ground network," *Elect. Lett.*, vol. 53, no. 13, pp. 885–887, Jun. 2017.

[25] D. Yang, Q. Wu, Y. Zeng, and R. Zhang, "Energy tradeoff in ground-to-UAV communication via trajectory design," *IEEE Trans. Veh. Technol.*, vol. 67, no. 7, pp. 6721–6726, Jul. 2018.

[26] Y. Xu, L. Xiao, D. Yang, L. Cuthbert, and Y. Wang, "Energy-efficient UAV communication with multiple GTs based on trajectory optimization," *Mobile Inf. Syst.*, vol. 2018, Apr. 2018, Art. no. 5629573.

[27] S. Boyd and L. Vandenberghe, *Convex Optimization*. Cambridge, U.K.: Cambridge Univ. Press, 2004.

[28] M. Grant and S. Boyd. (2016). *CVX: MATLAB Software for Disciplined Convex Programming*. [Online]. Available: https://cvxr.com/cvx

YU XU received the B.S. degree from the Information Engineering School, Jiangxi University of Science and Technology, Ganzhou, China, in 2015. He is currently pursuing the master's degree with the Information Engineering School, Nanchang University. His research interests include unmanned aerial vehicle communications and wireless resource management.

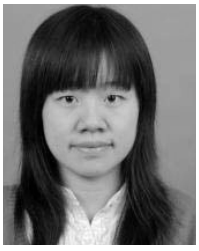

LIN XIAO received the Ph.D. degree from the School of Electronic Engineering and Computer Science, Queen Mary University of London, in 2010. After that, she was with the China Academy of Telecommunication Research of MITT for one year. She is currently an Associate Professor with the Information Engineering School, Nanchang University. Her research interests include wireless communication and networks, in particular, radio network planning and optimization, radio resource management, relay network, and cooperation communication.

DINGCHENG YANG received the Ph.D. degree in space physics from Wuhan University in 2012. He is currently an Associate Professor with the Information Engineering School, Nanchang University. His research interests are cooperation communications, cognitive radio techniques, and wireless resource management.

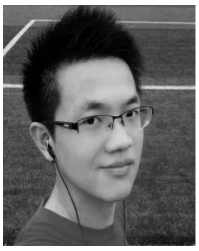

QINGQING WU (S'13–M'16) received the B.Eng. degree in electronic engineering from the South China University of Technology, China, in 2012, and the Ph.D. degree in electronic engineering from Shanghai Jiao Tong University (SJTU), China, in 2016. From 2015 to 2016, he was a Visiting Research Scholar with the School of Electrical and Computer Engineering, Georgia Institute of Technology, Atlanta, GA, USA. He received the IEEE WCSP Best Paper Award in 2015. His research interests include convex and nonconvex optimization, energy-efficient wireless communications, and unmanned aerial vehicle communications. He served as a TPC Member of the IEEE ICC 2017, GLOBECOM 2016, and ICC 2016. He was also a recipient of outstanding Ph.D. thesis funding in SJTU in 2016. He served as an Exemplary Reviewer of the IEEE COMMUNICATIONS LETTERS in 2016 and 2017, the IEEE TRANSACTIONS ON COMMUNICATIONS in 2017, and the IEEE TRANSACTIONS ON WIRELESS COMMUNICATIONS in 2017.

LAURIE CUTHBERT received the B.Sc. (Eng.) and Ph.D. degrees in electrical engineering from the University of London. He has also been a Visiting Professor with the Beijing University of Posts and Telecommunications, Dublin City University, and the Macao Polytechnic Institute. He is currently a Full Professor with the Queen Mary University of London (QMUL), where is a Special Adviser to the Principal on China Operations. He is also the Director of QMUL subsidiary companies in China. His research interests include telecommunications, particularly now in wireless communications. He has played an active role in EU research projects, leading international projects in the areas of ATM and then wireless communications. He is a Chartered Engineer and a fellow of the Institution of Engineering and Technology and received the Rayleigh Book Award for his book on ATM.